Comparison of 3D data acquisition methods for wound size assessment in crisis situations

Jakub Osuchowski[1,*,†], Rafał Gasz[1,†], Barbara Jantos[1,†] and Michał Wierzbicki[1,†]

[1] Opole University of Technology, Prószkowska 76 St., Opole, 45-758, Poland

Abstract

This study evaluates the feasibility of using the LiDAR sensor of the iPhone 16 Pro Max with the Zappcha application for contactless wound size assessment. A synthetic wound was scanned using three acquisition methods at three distances (25 cm, 50 cm, and 100 cm), and the resulting 3D reconstructions were compared with manual measurements. The findings show that scanning distance and device orientation strongly affect accuracy, with the best results obtained at 25 cm using stable acquisition paths. These results highlight the potential of smartphone-based LiDAR for rapid and reliable wound measurement in medical training, telemedicine, and emergency scenarios, while underlining the need for further validation in clinical practice.

Keywords

LiDAR, Crisis management, 3D modeling, 3D scanning, Computer Vision

1. Introduction

Humans perceive the world in three dimensions; we take it for granted and don't think about it. Replicating this natural ability in the digital realm has revolutionised cultural preservation [1], enhanced urban planning [2], and allowed the creation of autonomous vehicles [3]. Light Detection and Ranging (LiDAR) has emerged as one of the frontrunners in the field. LiDAR technology was first introduced in the 1960s. It relies on shooting a laser on the target and measuring reflected light, measuring differences in wavelength, and the time delta of the procedure [4]. Since then, the technology has managed to scale down from military-grade equipment to a part of mobile devices. Subsequently, it was employed in many more aspects of science, like robotics and everyday life, by being present in modern mobile phones. Moreover, recent experiments found it to be an effective and lightweight alternative to robust systems in the field of geomatics [5].

Recent achievements and the availability of LiDAR technology have made it possible to utilise it beyond industrial applications. Medicine is always looking for new ways to improve the care of patients, employing technological developments on a regular basis [6]. At the intersection of robotics and medicine, there is a thriving field of medical robots, easing the work of healthcare personnel. Recently, scientists experimented with a service robot with a 3D LiDAR system capable of autonomous navigation and operating within a medical environment [7]. Nonetheless, applications of LiDAR stretch even further into the medical domain. Thanks to mobile devices, the availability of such powerful technology opens up the possibility of incorporation in emergency scenarios, where robust equipment is unavailable.

Crisis Informatics and Emergency Medical Technologies are branches of science focused on actions, solutions, and equipment in extreme situations. In scenarios where assessment of the victims has to be made on the spot, such developments can be life-saving. Recently, a team of researchers from the Republic of Korea made progress in measuring the size of the wounds using LiDAR [8].

Although it was done under a controlled environment in a hospital, they managed to showcase a solution that is simple yet effective, especially in cases of wounds with irregular shapes.

In this article, the Authors focus on evaluating methods and parameters of data acquisition using LiDAR technology in smartphones in scenarios outside the hospital. The goal is to examine whether or not this is a feasible way of estimating wound sizes outside hospital halls and under uncertain, undetermined conditions. To achieve this goal, the authors have conducted experiments testing three methods and three different approaches to performing scans. The obtained results were compared and evaluated to estimate the best-performing one in terms of error rate in three dimensions of the artificial wound - length, width, and depth. Experiments utilise a commonly available smartphone with LiDAR capabilities, scanning an artificial wound in a non-sterile environment, simulating crisis scenarios.

2. Non-invasive measurement technologies

The development of measurement technologies in recent times has significantly increased the accuracy, speed, and accessibility of systems for acquiring spatial data.

In particular, there has been a dynamic increase in the use of non-contact methods that enable rapid mapping of object geometry in the form of three-dimensional models. These technologies are used in many fields – from reverse engineering, robotics, geoinformation and augmented reality. Systems enabling real-time 3D data acquisition with high accuracy and the ability to operate in various environmental conditions are of particular importance.

The most critical modern methods of spatial data acquisition include: digital photogrammetry, structured light, Time-of-Flight (ToF), and LiDAR [9, 10, 5]. Each of these technologies has its own specificity, advantages, and limitations.

Digital photogrammetry using the Structure from Motion (SfM) method allows 3D space reconstruction based on a set of photographs taken from different viewpoints. This process involves identifying characteristic points, matching them between images, and then estimating the positions and orientations of the cameras, which leads to the generation of first a sparse and later a dense 3D point cloud. Although this method is relatively inexpensive and can work using smartphones, its accuracy depends heavily on lighting conditions and object texture, and it also requires significant computational resources [11, 12, 13, 14].

In controlled conditions, SfM can achieve centimetre-level accuracy or better using a large number of high-resolution images, although its reliability decreases when surfaces are poorly textured or dimly lit, affecting point cloud density and reconstruction quality [12, 15]. Experiments with smartphones have shown that practical mobile SfM methods can generate models with accuracy comparable to professional scanners in applications such as terrain erosion monitoring or architectural measurements [16, 14]. An advantage of this method is the ability to use standard digital cameras and achieve high mapping accuracy, provided that proper lighting and well-varied surface textures are ensured. The drawbacks remain the time-consuming process and high computational demand, as well as susceptibility to errors in the case of homogeneous, shiny, or transparent surfaces.

Structured light technology is based on projecting a light pattern onto the surface of an object and analysing the deformation of that pattern using a camera that records the scene. Distortions in the pattern structure, resulting from interaction with the 3D geometry of the object's surface, enable precise determination of the surface shape. Structured light systems are based on the principle of geometric triangulation, where the positions of the projector and camera are known, and point depth is determined based on the angular difference between emitted and received rays. An advantage of this technology is the ability to achieve very high measurement precision, often in the micrometre range, and to generate dense point clouds with high spatial resolution. Thanks to this, structured light techniques are widely used in applications requiring high precision, such as manufacturing, industrial metrology, quality control, cultural heritage reconstruction, or biomedicine [17, 18, 19]. Despite many advantages, structured light systems also have limitations. The most important is sensitivity to lighting conditions – bright ambient light can disturb the visibility of the pattern, negatively impacting reconstruction quality. Additionally, scanning dark or shiny surfaces can lead to data loss or artefacts in the 3D model. This technology also typically has a limited operating range, making it best suited for short-distance measurements in controlled environments [20, 21, 22].

Time-of-Flight (ToF) camera technology is a dynamically developing method of depth data acquisition, based on measuring the travel time of light between the sensor and the object's surface.

In classical ToF systems, the detector measures the time it takes for an emitted light pulse (usually in the near-infrared range) to travel to the object and back. In practical versions, sinusoidally modulated continuous light is most commonly used, and the distance is determined based on the phase shift between the sent and received signal [23]. One of the key advantages of ToF cameras is the ability to generate depth data in real-time, making them an attractive solution in mobile, robotic, and interactive applications. Thanks to their compact design, they can be easily integrated with portable devices such as smartphones or augmented reality systems [24]. ToF cameras show low dependency on object texture and colour, allowing their use in visually diverse environments, including uniformly colored or poorly lit surfaces. However, this technology is not without limitations. High sensitivity to photon noise and light interference can affect data quality, especially under intense lighting or at long distances [23, 25]. An additional problem is the low spatial resolution compared to other 3D acquisition methods, such as photogrammetry or structured light, which limits the ability to reconstruct fine details [25]. Moreover, in the case of highly reflective or transparent objects, ToF systems may produce distorted depth data, requiring additional correction algorithms [23].

LiDAR technology is currently one of the most advanced solutions in the field of spatial measurements. Its operating principle is based on the emission of light pulses, most often in the near-infrared range, which, after reflecting from objects, return to the detector. The time of flight of the pulse, measured with high precision, allows the distance to the object to be determined [26]. Thanks to the very high frequency of pulse emission, LiDAR systems can generate millions of points per second, creating extremely dense and accurate point clouds. An advantage of this technology is its independence from lighting conditions and the ability to operate both day and night [23]. Additionally, LiDARs handle mapping complex, irregular shapes and structures well, including in natural and urban environments. In recent years, there has been a miniaturisation of these systems and their integration with mobile devices, significantly increasing the accessibility of this technology for field applications [5]. The miniaturisation of LiDAR systems has enabled their integration with portable devices (e.g., iPhone Pro, iPad Pro, some Android models), as well as with drones and inspection robots [5, 23]. As a result, measurements can be taken in real time without the need for heavy equipment. Despite many advantages, LiDAR technology is associated with higher equipment costs, the need to process large amounts of data, and the requirement for precise calibration in more complex measurement configurations.

3. LiDAR-Based Wound Assessment

During crisis situations such as rescues after natural disasters, terrorist attacks, or on the battlefield, it is crucial to assess wounds quickly, objectively, and contactlessly. Traditional methods of wound assessment based on rulers and subjective staff judgment are time-consuming, prone to errors, and not always feasible, especially in field conditions. In response to these needs, there is active development of systems that use 3D scanning with LiDAR technology, often supported by artificial intelligence and computer vision methods, which allow quick and precise reproduction of wound structure without the need for physical contact.

Before the technology can be deployed in the field, it has to be tested in labs and hospitals. Such clinical trials were conducted by Liu et al. [27]. Using LiDAR technology implemented in devices such as the iPhone 12 Pro or iPad Pro to measure the area of wounds, they compared its accuracy to measurement results obtained using the ruler method and digital analyses done with ImageJ. The results achieved with the app using LiDAR surpassed the traditional method for pressure injury assessment. However, it is underlined that deep wounds could be mismeasured.

Similarly, another limitation was pointed out in [8], where surgical wounds smaller than 2.0 × 2.0 cm² were excluded from the study due to the technical limitations of LiDAR in smartphone devices. However, it was still possible to develop a ready-to-use app that measures the wound area. The correlation between the results achieved by the app and ImageJ analysis was 0.995, which is a promising result for practitioners, enabling them to measure wounds contactlessly and thus lowering the risk of wound infection.

Next example of LiDAR technology usage is the WounDAR platform (Wound Detection and Assessment using Range and Vision) developed by Akeboshi et al. [28]. It is also available on consumer-level mobile devices, which presents great potential for field operations. The method uses a LiDAR sensor, an RGB camera, and deep neural networks for wound analysis – it not only focuses on size but also considers wound localisation, segmentation, and tissue classification. The system was

developed and tested on photos of injuries at different stages and of various origins, including ulcers, surgical wounds, and pressure ulcers. However, the results showed that, for the proposed platform, using the iPhone 12 LiDAR camera does not guarantee achieving the required sensor accuracy to achieve an acceptable error level.

The significance of depth measurement is highlighted in [29], where the authors presented a system combining a deep learning model with LiDAR technology for assessing the area and depth of burns—Burn Evaluation Network. Thanks to LiDAR sensors, a 3D map of the wound can be reconstructed while preserving wound geometry. The data, including the depth of injuries, was manually annotated by clinicians for further model training. The authors point out that 2D measurements tend to underestimate wound area; therefore, it is crucial to include 3D measurements in contactless wound sizing.

In [30], a mobile LiDAR system (Time-of-Flight sensor) combined with an RGB camera was proposed for wound assessment. The study utilised both synthetically generated images and images captured from wound phantoms designed to replicate surgical wounds and ulcers. The Time-of-Flight sensor was used to measure the distance to the skin surface, while the RGB camera provided information about the shape and colour of the wounds. Although the authors developed a regression model that achieved an error of less than 5% relative to the actual wound size, the method was not evaluated in real-world clinical scenarios.

LiDAR-based technologies, especially when combined with AI models, hold great promise for innovation in contactless wound size assessment, particularly under challenging conditions. However, issues such as the accurate measurement of deep wounds and poor lighting conditions still need to be addressed. Moreover, these solutions must be validated in clinical settings using large, real-world datasets.

4. Experiment Description

The aim of this experiment is to evaluate the accuracy and consistency of different 3D acquisition strategies for capturing the geometry of a synthetic wound using a mobile LiDAR sensor. The study was conducted with the iPhone 16 Pro Max equipped with a LiDAR scanner, in combination with the Zappcha mobile application for real-time point cloud generation.

To assess the influence of acquisition technique on the quality of wound reconstruction, a total of nine point clouds were collected. The scanning process was performed in continuous mode by rotating the joint around the wound to capture its shape from all angles. Three distinct acquisition methods were applied, each differing in the orientation and rotation path of the device relative to the wound surface. Additionally, each method was executed at three different distances: 25 cm, 50 cm, and 100 cm.

The collected data was processed in CloudCompare, where key wound dimensions—length (x), width (y), and depth (z)—were extracted and compared. The goal of the experiment is to determine which combination of orientation and distance yields the most precise and reliable 3D wound representation.

Figure 1 presents the synthetic wound used throughout the study, with the three key spatial dimensions annotated: length (x), width (y), and depth (z). These measurements serve as the reference values for evaluating the accuracy of the 3D reconstructions obtained through various acquisition methods.
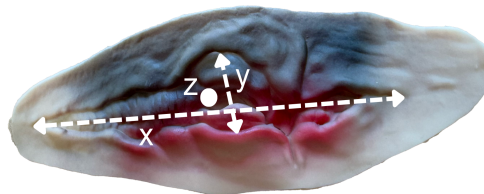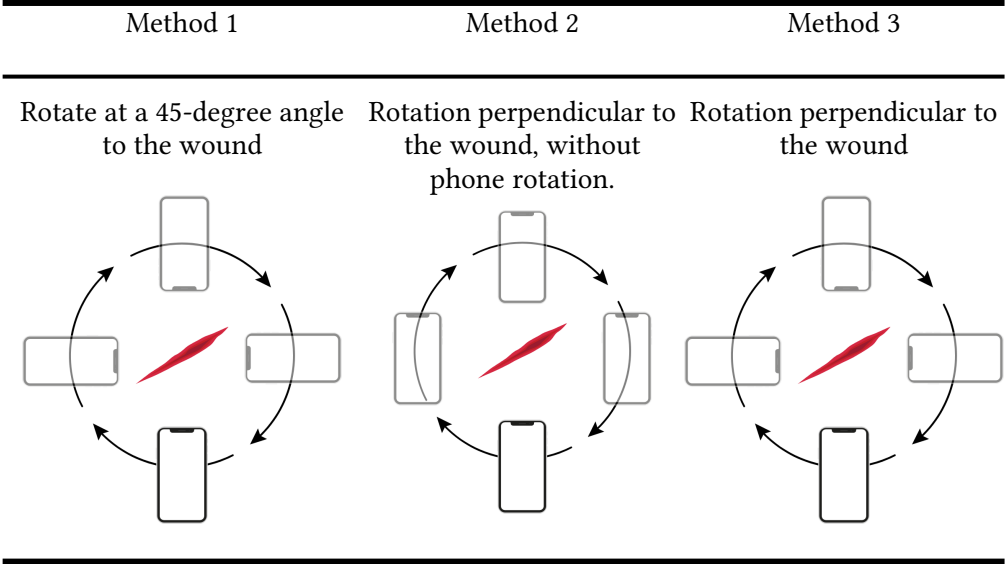

Figure 1: Artificial wound with annotated dimensions: length (x) = 13.72 cm, width (y) = 2.64 cm, depth (z) = 0.45 cm.

Table 1 provides a visual summary of the three device orientation strategies applied during

the scanning process. The diagrams illustrate how the phone was positioned and rotated around the wound in each method.

Table 1

Visualization of three acquisition methods for 3D wound scanning using the iPhone 16 Pro Max and the Zappcha app.

Method 1	Method 2	Method 3
Rotate at a 45-degree angle to the wound	Rotation perpendicular to the wound, without phone rotation.	Rotation perpendicular to the wound

In all methods, the scanning was performed in continuous mode by rotating the joint around the wound, while keeping the phone orientation fixed. The methods differ in the angle and path of device rotation relative to the wound:

- Method 1 involves holding the phone at a 45-degree angle to the wound.
- Method 2 also keeps the phone perpendicular, without phone rotation.
- Method 3 keeps the phone perpendicular to the wound, with rotation performed horizontally around the target.
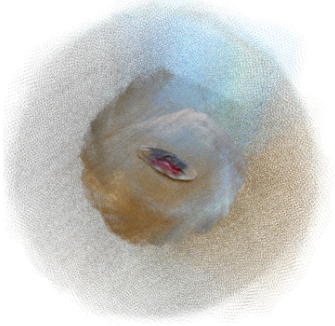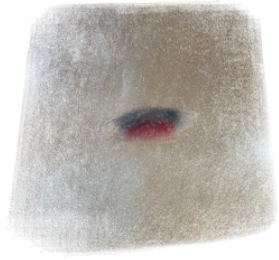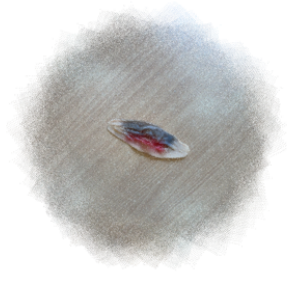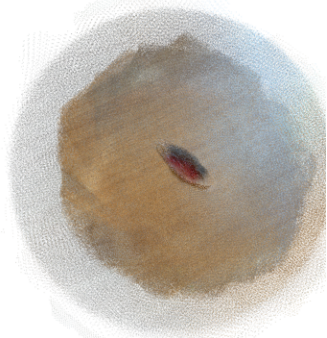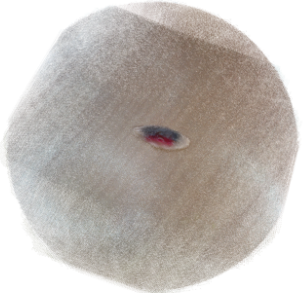
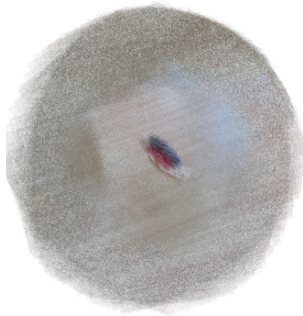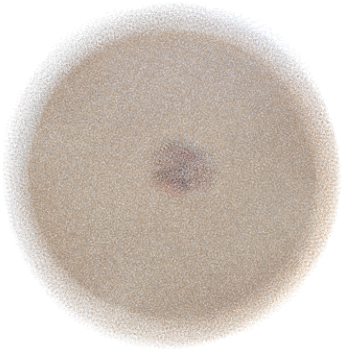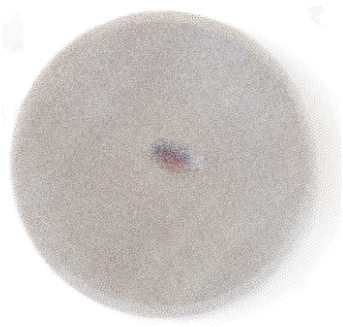These approaches were designed to evaluate how different spatial orientations during acquisition affect the accuracy and completeness of the resulting 3D reconstructions.

5. Results

The main objective of this study was to assess the influence of different acquisition methods and distances on the accuracy of 3D wound reconstruction. After collecting a total of nine point clouds using the three predefined acquisition strategies at varying distances (25 cm, 50 cm, and 100 cm), the resulting data were analyzed using CloudCompare software.

The point clouds obtained during the study are presented in Table 2.

Table 2
Point Cloud Obtained During the Study

Distance	Method 1	Method 2	Method 3
25 cm			
50 cm			
100 cm			

The key spatial dimensions of the wound—length (x), width (y), and depth (z)—were extracted for each configuration. The results were then compared against the reference measurements obtained directly from the physical wound model. This comparison allows for an evaluation of how closely each 3D reconstruction matches the true dimensions and which configuration yields the most reliable results.

Table 3 presents the dimensional values (in centimeters) extracted from each of the nine acquired point clouds. The results are organized by acquisition method and scanning distance. The first row includes the manually obtained reference values, serving as the ground truth for all subsequent comparisons.

Table 3
Point Cloud Obtained During the Study

Method	Distance(cm)	x (cm)	y (cm)	z (cm)
Reference	–	13.72	2.64	0.45
Method 1	25.00	13.38	2.81	0.3
Method 2	25.00	12.34	3.34	0.21
Method 3	25.00	13.81	2.47	0.5
Method 1	50.00	12.45	3.69	0.22
Method 2	50.00	12.28	3.29	0.26
Method 3	50.00	12.71	3.72	0.23
Method 1	100.00	14.86	10.32	0.33
Method 2	100.00	12.61	3.92	0.14
Method 3	100.00	9.23	4.53	0.17

The results in Table 3 indicate that none of the tested acquisition methods produced a perfect match with the reference measurements across all three dimensions. However, certain trends can be observed:

- Method 1 generally produced stable length (x) measurements, especially at 25 cm and 50 cm, though some overestimation occurred at 100 cm.
- Method 2 yielded relatively consistent results across distances, with moderate accuracy in all three dimensions. Notably, depth (z) was underestimated in all cases.
- Method 3 showed the greatest variability, especially at 100 cm, where all dimensions deviated significantly from the reference, particularly width (y).

Overall, the 25 cm distance yielded the most accurate and visually interpretable results across methods, likely due to higher point density and better surface detail capture. Among all scans, the wound was most clearly visible and easiest to interpret in the point clouds obtained using Method 1 and Method 3 at 25 cm.

Figure 2 presents the measured values of the wound's length (x), width (y), and depth (z) obtained from 3D point clouds acquired using different methods and distances. Each bar represents a specific acquisition configuration, and the red dashed line indicates the manually measured reference value for that dimension.
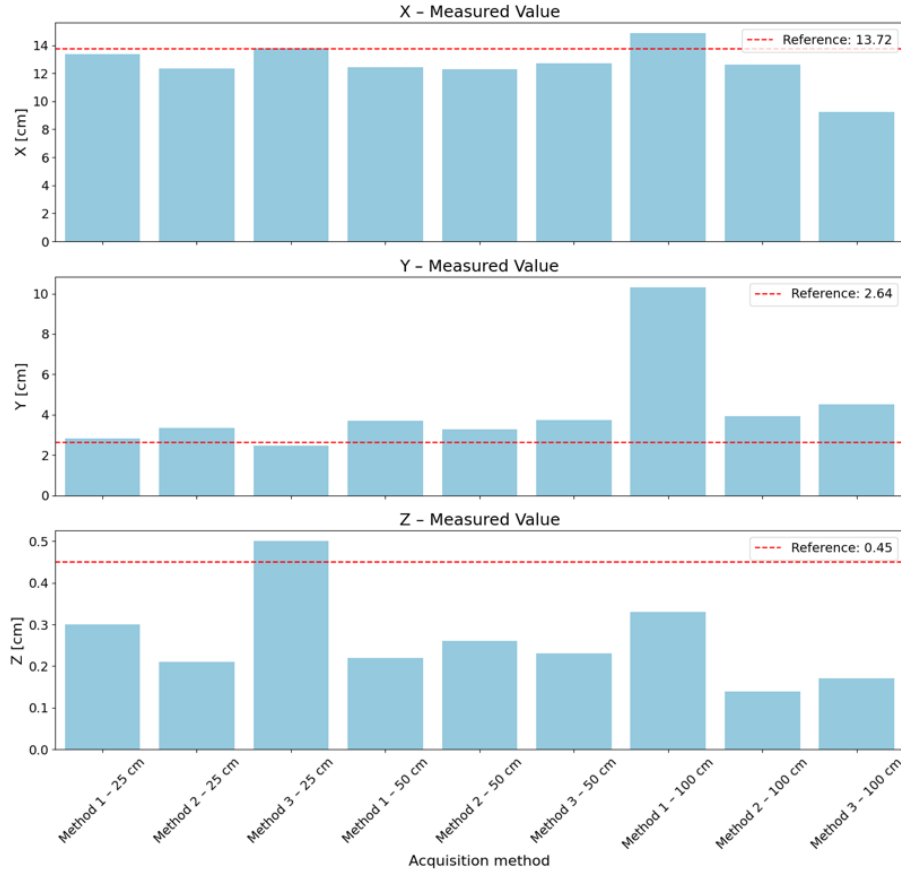
Figure 2: Comparison of measured wound dimensions (x, y, z) from 3D point clouds across different acquisition methods and distances. The red dashed line represents the ground truth (reference measurement).

The results presented in Figure 2 show that most acquisition methods led to minor underestimation or overestimation of the wound's actual dimensions. Notably, Method 3 at a distance of 100 cm resulted in the largest deviations in both length and width. In contrast, measurements taken at a distance of 25 cm were consistently closer to the reference values. Among these, Method 1 and Method 3 yielded the most accurate results, suggesting that closer proximity to the wound, combined with specific device orientations, positively influences dimensional accuracy. Method 2 exhibited moderate stability across all distances but did not outperform the others at any point.

Figure 3 illustrates the relative error (%) for each of the measured wound dimensions (x, y, z), calculated with respect to the reference values. The relative error for each dimension was computed using the following formula:

$$Relative\ Error = \frac{Measured\ Value - Reference\ Value}{Reference\ Value} \times 100\ \%$$ (1)
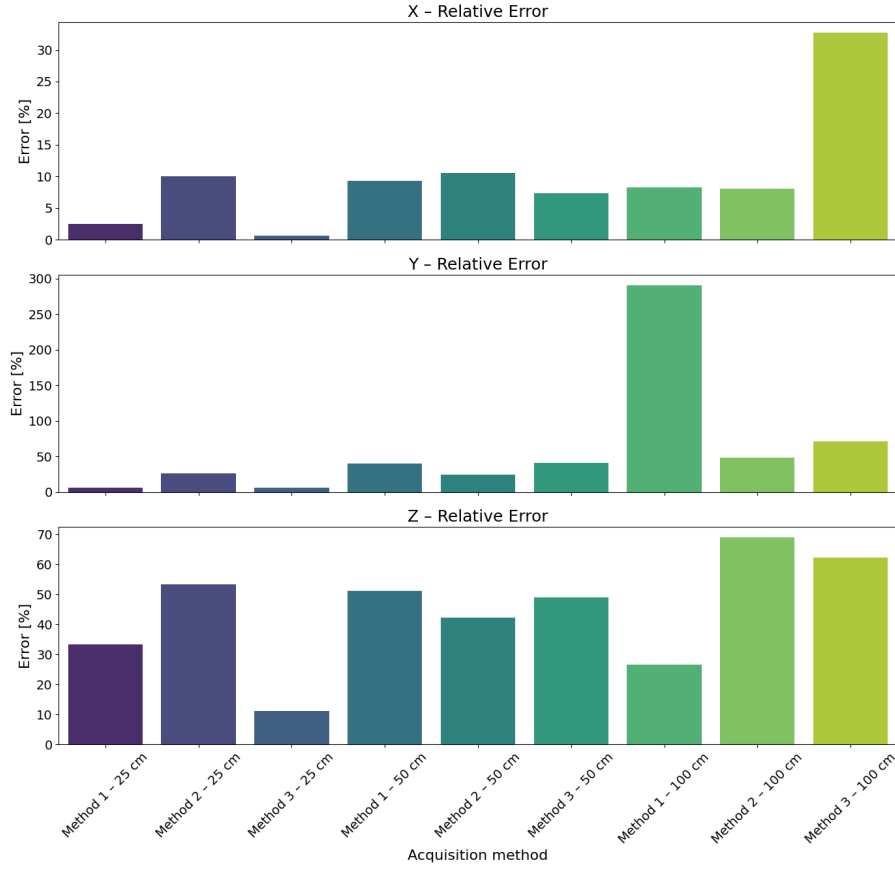
Figure 3: Relative errors in the measured wound dimensions (x, y, z) for each acquisition configuration. Lower values indicate higher accuracy of 3D reconstruction.

As illustrated in Figure 3, the depth dimension (z) was generally the worst reconstructed across all methods and distances. The width (y) showed considerable variability, particularly in the case of Method 1 at 100 cm, where the error reached its peak. The lowest relative errors were observed for Method 1 and Method 3 at a scanning distance of 25 cm, indicating that close-range acquisition not only improves measurement accuracy but also minimizes variability. In contrast, Method 3 at 100 cm consistently produced high relative errors across all dimensions, demonstrating the limitations of distant scanning with that orientation.

Figure 4 presents a heatmap showing the total relative error, calculated as the sum of the individual relative errors for length (x), width (y), and depth (z). This aggregated error metric helps identify which acquisition strategies performed best overall. The total relative error was computed as:

$$Total\ Relative\ Error = \left(\frac{|x_m - x_r|}{x_r} + \frac{|y_m - y_r|}{y_r} + \frac{|z_m - z_r|}{z_r} \right) \times 100\ \% \qquad (2)$$

Where:
- x_m, y_m, z_m – values of the wound's length, width, and depth obtained from the 3D point cloud (measured values)
- x_r, y_r, z_r – manually measured reference values for the wound's length, width, and depth
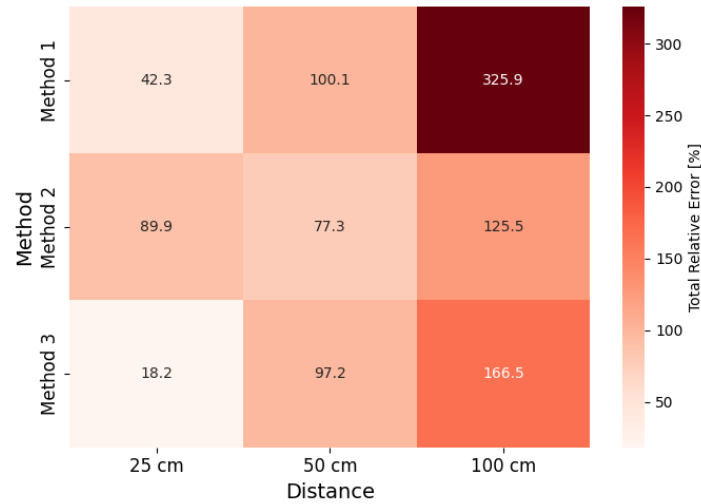
Figure 4: Relative errors in the measured wound dimensions (x, y, z) for each acquisition configuration. Lower values indicate higher accuracy of 3D reconstruction.

The heatmap in Figure 4 provides a comprehensive overview of total reconstruction error across all acquisition strategies. The best-performing configuration was Method 3 at 25 cm, closely followed by Method 1 at the same distance. These configurations yielded the lowest cumulative errors in all three dimensions. Conversely, Method 1 at 100 cm resulted in the highest total error, primarily due to substantial overestimation of wound width. Overall, the data strongly indicate that shorter acquisition distances lead to more precise and consistent 3D reconstructions, regardless of the specific method employed.

6. Conclusion

This study evaluated the accuracy of 3D wound reconstruction using the LiDAR sensor of the iPhone 16 Pro Max in combination with the Zappcha application. Three acquisition methods, each applied at three distances, were tested by capturing point clouds of a synthetic wound. The dimensional measurements extracted from these reconstructions were compared against reference values obtained through manual measurement.

The results clearly indicate that both the acquisition distance and the device orientation play a significant role in the quality of 3D data. The most accurate and visually interpretable reconstructions were obtained at a distance of 25 cm, particularly with Method 1 and Method 3. In contrast, increased distance — especially 100 cm — significantly reduced reconstruction fidelity, often leading to high relative errors, especially in wound width.

Overall, close-range scanning combined with stable device orientation proved to be the most effective strategy. These findings can guide future applications of smartphone-based 3D scanning in medical simulation, training, or telemedicine. Further work will focus on optimizing the scanning path and evaluating reconstruction quality in real-world clinical scenarios.

7. Future Works

Future work should systematically test a more comprehensive array of methods and corresponding parameters. Current findings should be expanded by conducting tests on a broader range of wound types, anatomical locations, and patient populations, which would ensure the robustness of the data collected. Furthermore, a comparison between different devices is also advised to achieve a sense of universality of the results. Finally, developing a standardized procedure that would ensure the best results with ease of performance should become a long-term goal.

8. Limitations

This study has several important limitations that should be addressed. First of all, tests were conducted using a fake wound. While it is understandable to use a prop, it still does not reflect the variety of other types of wounds or the inherent realness of the injury. The experiment setup considered only a few of the possible configurations, which again might not correlate to a real-world setting. Subtle changes in lighting, angle, movement speed, or distance can greatly affect the outcome. All data comes from one device, which might hinder the application of the results in the general case.

Declaration on Generative AI

The author(s) have not employed any Generative AI tools.

References

[1] A. Crisan, M. Pepe, D. Costantino, S. Herban, From 3d point cloud to an intelligent model set for cultural heritage conservation, Heritage 7 (2024) 1419–1437. URL: https://www.mdpi.com/2571-9408/7/3/68. doi:10.3390/heritage7030068.

[2] T. R. Andersen, S. E. Poulsen, M. A. Pagola, A. B. Medhus, Geophysical mapping and 3d geological modelling to support urban planning: A case study from vejle, denmark, Journal of Applied Geophysics 180 (2020) 104130. URL: https://www.sciencedirect.com/science/article/pii/S0926985120300781. doi:https://doi.org/10.1016/j.jappgeo.2020.104130.

[3] A. Ghasemieh, R. Kashef, 3d object detection for autonomous driving: Methods, models, sensors, data, and challenges, Transportation Engineering 8 (2022) 100115. URL: https://www.sciencedirect.com/science/article/pii/S2666691X22000136. doi:https://doi.org/10.1016/j.treng.2022.100115.

[4] N. Mehendale, S. Neoge, Review on lidar technology, Preprint, SSRN Electronic Journal (2020). URL: https://ssrn.com/abstract=3604309. doi:10.2139/ssrn.3604309, preprint, not peer-reviewed.

[5] S. Zollini, L. Marconi, Evaluation of positioning accuracy using smartphone rgb and lidar sensors with the vidoc rtk rover, Sensors 25 (2025). URL: https://www.mdpi.com/1424-8220/25/13/3867. doi:10.3390/s25133867.

[6] A. Haleem, M. Javaid, R. Pratap Singh, R. Suman, Medical 4.0 technologies for healthcare: Features, capabilities, and applications, Internet of Things and Cyber-Physical Systems 2 (2022) 12–30. URL: https://www.sciencedirect.com/science/article/pii/S2667345222000104. doi:https://doi.org/10.1016/j.iotcps.2022.04.001.

[7] S. Ibrayev, A. Ibrayeva, B. Amanov, S. Tolenov, Development of a service robot for hospital environments in rehabilitation medicine with lidar-based simultaneous localization and mapping, International Journal of Advanced Computer Science and Applications 15 (2024). URL: http://dx.doi.org/10.14569/IJACSA.2024.01511102. doi:10.14569/IJACSA.2024.01511102.

[8] B. Song, J. Kim, H. Kwon, S. Kim, S.-H. Oh, Y. Ha, S.-H. Song, Smartphone-based lidar application for easy and accurate wound size measurement, Journal of Clinical Medicine 12 (2023) 6042. URL: https://doi.org/10.3390/jcm12186042. doi:10.3390/jcm12186042.

[9] F. M. Sheshtar, et al., Comparative analysis of lidar and photogrammetry for mobile-based mapping technologies, Applied Sciences 15 (2025). doi:10.3390/app15031085.

[10] R. Maskeliūnas, et al., Fusing lidar and photogrammetry for accurate 3d data, Remote Sensing 17 (2025). doi:10.3390/rs17030443.

[11] J. Shan, et al., Democratizing photogrammetry: an accuracy perspective, International Journal of Applied Earth Observation and Geoinformation (2023). doi:10.1080/10095020.2023.2178336.

[12] M. Nielsen, et al., Quantifying the influence of surface texture and shape on reconstruction accuracy in structure from motion, Sensors 23 (2022) 178. doi:10.3390/s23010178.

[13] E. Heng Siong, M. Ariff, A. Razali, The application of smartphone-based structure from motion (sfm) photogrammetry in ground volume measurement, International Archives of the Photogrammetry, Remote Sensing and Spatial Information Sciences XLVIII-4/W6 (2023) 145–152. doi:10.5194/isprs-archives-XLVIII-4-W6-2023-145-2023.

[14] L. Teixeira Coelho, et al., Evaluating the accuracy of smartphone-based photogrammetric methods for 3d facial modeling, Symmetry 17 (2025) 376. doi:10.3390/sym17030376.

[15] F. Roza de Moraes, I. da Silva, Optimizing submillimeter 3d modeling with auxiliary lighting and artificial textures: An sfm-based approach, F1000Research 13 (2024) 1479. doi:10.12688/f1000research.157676.1.

[16] S. Tavani, et al., Terrestrial sfm-mvs photogrammetry from smartphone sensors: case study on a geological cliff, International Journal of Applied Earth Observation and Geoinformation 89 (2020) 102093. doi:10.1016/j.jag.2020.102093.

[17] J. Geng, Structured-light 3d surface imaging: a tutorial, Advances in Optics and Photonics 3 (2011) 128–160. doi:10.1364/AOP.3.000128.

[18] B. Cui, W. Tao, H. Zhao, High-precision 3d reconstruction for small-to-medium-sized objects utilizing line-structured light scanning: A review, Remote Sensing 13 (2021) 4457.

[19] X. Wei, S. Zhang, F. Gao, Review of structured light techniques for 3d shape measurement, Optics and Lasers in Engineering 154 (2022) 107090. doi:10.1016/j.optlaseng.2022.107090.

[20] J. Salvi, S. Fernandez, T. Pribanic, X. Llado, A state of the art in structured light patterns for surface profilometry, Pattern Recognition 43 (2010) 2666–2680. doi:10.1016/j.patcog.2009.12.004.

[21] Z. Zhang, P. S. Huang, Recent progress in structured light-based three-dimensional scanning, Optics and Lasers in Engineering 106 (2018) 119–131. doi:10.1016/j.optlaseng.2017.12.003.

[22] Y. Wang, X. Chen, L. Zhang, Structured light 3d imaging: A review of recent developments and applications, IEEE Transactions on Instrumentation and Measurement (2023). doi:10.1109/TIM.2023.3248291.

[23] J. Ma, W. Zhang, P. Liu, A review of tof-based lidar: Principles, challenges and applications, Journal of Semiconductors 45 (2024) 104002. doi:10.1088/1674-4926/45/10/104002.

[24] T. Schöps, T. Sattler, M. Pollefeys, Bad slam: Bundle adjusted direct rgb-d slam, Proceedings of the IEEE/CVF Conference on Computer Vision and Pattern Recognition (2019) 134–144.

[25] Y. Chen, K. Qian, X. Cheng, J. Zhou, A learning method to optimize depth accuracy and frame rate for time of flight camera, in: IOP Conference Series: Materials Science and Engineering, volume 563, IOP Publishing, 2019, p. 042067.

[26] A. Wehr, U. Lohr, Airborne laser scanning—an introduction and overview, ISPRS Journal of Photogrammetry and Remote Sensing 54 (1999) 68–82. doi:10.1016/S0924-2716(99)00011-8.

[27] T. J. Liu, H. Wang, M. Christian, C.-W. Chang, F. Lai, H.-C. Tai, Automatic segmentation and measurement of pressure injuries using deep learning models and a lidar camera, Scientific Reports 13 (2023). doi:10.1038/s41598-022-26812-9.

[28] W. Naoto, M. T. Cotoco, R. C. Balajadia, L. T. Lim, A. Ken, R. A. Bedruz, A. Sy, C. Ramos, Woundar: Lidar and machine vision based wound assessment, 2021 IEEE 13th International Conference on Humanoid, Nanotechnology, Information Technology, Communication and Control, Environment, and Management (HNICEM) (2022) 1–6. URL: https://ieeexplore.ieee.org/document/10109427. doi:10.1109/hnicem57413.2022.10109427.

[29] C. W. Chang, H. Wang, F. Lai, M. Christian, S. Chen Huang, H. Yi Tsai, Comparison of 3d and 2d area measurement of acute burn wounds with lidar technique and deep learning model, Frontiers in Artificial Intelligence 8 (2025). doi:10.3389/frai.2025.1510905.

[30] S. B. Wibowo, A. A. Nugroho, L. Awaludin, L. Hidayat, Regression model for measurement of wound dimensions by webcam scanners and time-of-flight sensors, 2025. URL: https://arxiv.org/abs/2504.04727. arXiv:2504.04727.